

# Phase Diagram of $\text{Ba}_2\text{NaOsO}_6$ , a Mott insulator with strong spin orbit interactions

W. Liu, R. Cong, E. Garcia

*Department of Physics, Brown University, Providence, RI 02912, U.S.A.*

A. P. Reyes

*National High Magnetic Field Laboratory, Tallahassee, FL 32310, U.S.A.*

H. O. Lee

*Department of Applied Physics and Geballe Laboratory for Advanced Materials, Stanford University, California 94305, U.S.A*

I. R. Fisher

*Department of Applied Physics and Geballe Laboratory for Advanced Materials, Stanford University, California 94305, U.S.A*

V. F. Mitrović\*

*Department of Physics, Brown University, Providence, RI 02912, U.S.A.*

---

## Abstract

We report  $^{23}\text{Na}$  nuclear magnetic resonance (NMR) measurements of the Mott insulator with strong spin-orbit interaction  $\text{Ba}_2\text{NaOsO}_6$  as a function of temperature in different magnetic fields ranging from 7 T to 29 T. The measurements, intended to concurrently probe spin and orbital/lattice degrees of freedom, are an extension of our work at lower fields reported in [1]. We have identified clear quantitative NMR signatures that display the appearance of a canted ferromagnetic phase, which is preceded by local point symmetry breaking. We have compiled the field temperature phase diagram extending up to 29 T. We find that the broken local point symmetry phase extends over a wider temperature range as magnetic field increases.

*Keywords:* Spin orbit coupling, Mott insulators, orbital order, quadrupolar order, anisotropic magnetic interactions

*PACS:* 75.30.-m, 75.25.-j, 75.25.Dk, 75.10.Jm

## 1. Introduction

The combined effects of strong electronic correlations with spin-orbit coupling (SOC) can lead to a plethora of emergent novel quantum states.

In the quest to predict and identify the emergent phases, studies have focused on magnetic Mott insulators with strong SOC [2, 3, 4, 5]. Strong SOC can significantly enhance quantum fluctuations and amplify effects of frustration leading to novel quantum states [3, 4, 6]. A key feature of theoretical models for predicting the emergent properties is that significant interactions are

---

\*Corresponding author

*Email address:* vemi@brown.edu (V. F. Mitrović)

fourth and sixth order in the effective spins, due to strongly orbital-dependent exchange [3].

The Mott insulating  $d^1$  double perovskites with cubic structure are model systems of Mott insulators with strong SOC. An example material is  $\text{Ba}_2\text{NaOsO}_6$ , a double perovskite with Na and Os ions inhabiting alternate cation B sites, which for an undistorted structure has a face-centered-cubic lattice. We have performed microscopic measurements designed to concurrently probe spin and orbital/lattice degrees of freedom in this compound and so provide stringent tests of theoretical approaches. Our static NMR measurements reveal that the local cubic symmetry breaking, induced by a deformation of the oxygen octahedra, precedes the formation of the long range ordered magnetism [1]. Specifically, we found that these deformations generate an orthorhombic point symmetry in the magnetic phase. Furthermore, we established that the magnetically ordered state is the canted two-sublattice ferromagnet (FM), believed to be driven by the staggered quadrupolar order [3]. Our observation of both the local cubic symmetry breaking and appearance of two-sublattice exotic FM phase is in line with theoretical predictions based on quantum models with multipolar magnetic interactions [3]. Thus, our findings establish that such quantum models with multipolar magnetic interactions represent an appropriate theoretical framework for predicting emergent properties in materials with both strong correlations and SOC, in general. To provide further tests of quantum models, here we present the extension of our work in Ref. [1] to high magnetic fields. We compile the field temperature phase diagram extending up to 29 T. We find that as magnetic field increases, broken local point symmetry phase extends over wider temperature range.

## 2. Experimental Technique and the Sample

The measurements were done at the NHMFL in Tallahassee, FL using both high homogeneity superconducting and resistive magnets. The temperature control was provided by  $^4\text{He}$  variable temperature insert. The NMR data was recorded

using a state-of-the-art laboratory-made NMR spectrometer. The spectra were obtained, at each given value of the applied field, from the sum of spin-echo Fourier transforms recorded at constant frequency intervals. We used a standard spin echo sequence  $(\pi/2 - \tau - \pi)$ . A gyromagnetic ratio of  $^{23}\gamma = 11.2625 \text{ MHz/T}$  was used for all frequency to field scale conversions. For nuclear sites with spin  $I > 1/2$ , such as  $^{23}\text{Na}$  with  $I = 3/2$ , and non-zero electric field gradient (EFG), quadrupole interaction between nuclear spin and EFG splits otherwise single NMR line to  $2I$  lines [7]. Thus, the  $^{23}\text{Na}$  spectral line splits in three in the presence of a non-zero EFG. However, for small finite values of the EFG three peaks are not necessarily discernible, in which case significant line broadening can only be detected. At sites with cubic point symmetry the EFG is zero, as is the case for Na nuclei in the high temperature PM phase, and a single line is observed.

The sample was both zero-field and field-cooled. We did not detect any influence of the sample's cooling history on the NMR spectra. Nevertheless for consistency, all results presented in the paper were obtained in field-cooled conditions. The sample was mounted to one of the crystal faces and rotated with respect to the applied field about an axis using a single axis goniometer. The direction perpendicular to the face to which the sample was mounted denotes [001] direction. The labeling is only relevant in the low temperature magnetically ordered phase characterized by orthorhombic point symmetry.

High quality single crystals of  $\text{Ba}_2\text{NaOsO}_6$  with a truncated octahedral morphology were grown from a molten hydroxide flux, as described in Refs. [8, 9]. Crystal quality was checked by x-ray diffraction, using a Bruker Smart Apex CCD diffractometer, which indicated that the room temperature structure belongs to the  $Fm\bar{3}m$  space group [9]. NMR measurements were performed for a single crystal with a volume of approximately  $1 \text{ mm}^3$ . Such a small sample volume precludes effective neutron scattering studies of magnetic order. The quality of the sample was confirmed by the sharpness of  $^{23}\text{Na}$  NMR spectra both in the high temperature paramagnetic state and low temper-

ature quadrupolar split spectra.

### 3. Temperature and Field Evolution of NMR Spectra

To determine the field-temperature phase diagram of  $\text{Ba}_2\text{NaOsO}_6$ , we inspect the temperature ( $T$ ) dependence of  $^{23}\text{Na}$  NMR spectra measured in applied magnetic fields ( $H$ ) that exceed those presented in Ref. [1]. In Fig. 1, we plot the temperature evolution of  $^{23}\text{Na}$  NMR spectra measured at four different magnetic fields ranging from 11 T to 29 T. The analysis of these  $^{23}\text{Na}$  spectra allows us to determine the transition temperature ( $T_c$ ) from paramagnetic to low temperature ferromagnetic state and the onset temperature for breaking of local cubic symmetry ( $T^*$ ), as described in sections below. This is because these spectra reflect the distribution of the hyperfine fields and the electronic charge and are thus a sensitive probe of both the electronic spin polarization (local magnetism) and charge distribution (orbital order and/or lattice symmetry).

High temperature spectra consist of a single narrow NMR line. Since the nuclear spin  $I$  of  $^{23}\text{Na}$  equals to  $3/2$ , the absence of the three distinct quadrupolar satellite lines indicates that EFG is zero as a consequence of a cubic environment. Therefore, the observed single narrow NMR spectra is evidence that the high temperature phase of  $\text{Ba}_2\text{NaOsO}_6$  is a PM state characterized by cubic symmetry. On lowering the temperature, the NMR line broadens and splits into multiple peaks indicating onset of significant changes in the local symmetry, thereby producing EFG, *i.e.* asymmetric (non-cubic) charge distribution. Therefore, the observed line broadening and subsequent splitting of the Na spectra into triplets, in the magnetically ordered phase, indicates breaking of the cubic point symmetry caused by local distortions of electronic charge distribution, as established in [1]. These distortions, marking the broken local point symmetry (BLPS) phase, occur above the transition into the magnetic state.

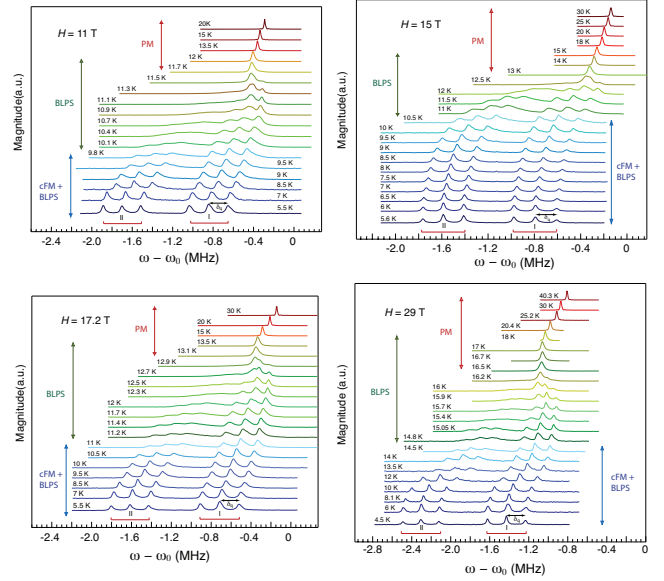


Figure 1: Temperature evolution of  $^{23}\text{Na}$  spectra at various strengths of magnetic field, applied parallel to  $[001]$  crystalline axis, as denoted. Narrow single peak spectra characterize high temperature paramagnetic (PM) state. At intermediate temperatures, broader and more complex spectra reveal the appearance of an electric field gradient (EFG) induced by breaking of local cubic symmetry, as described in [1]. Splitting into 2 sets of triplet lines (labeled as I and II), reflecting the existence of two distinct magnetic sites in the lattice, is evident at lower temperatures. Zero of frequency is defined as  $\omega_0 = ^{23}\gamma H$ . Splitting between quadrupolar satellites is denoted by  $\delta_q$ . Abbreviation: PM, paramagnetic; BLPS, broken local point (cubic) symmetry; and, cFM, canted ferromagnetic.

For example, at low temperatures below 10 K at 11 T, the  $^{23}\text{Na}$  spectra clearly split into 6 peaks, that is two sets of triplet lines, labeled as I and II in Fig. 1, that are well separated in frequency. The emergence of these two sets of triplets indicates the appearance of two distinct magnetic sites, *i.e.* two nuclear sites that sense two different local fields in the lattice, as described in [1]. More precisely, detailed analysis of the NMR spectra as a function of the strength and direction of the applied field revealed that the two sets of triplets originate from two-sublattice canted ferromagnetic phase [1]. Therefore, the two sets of triplet lines indicate the presence of the long range ordered (LRO) magnetism.

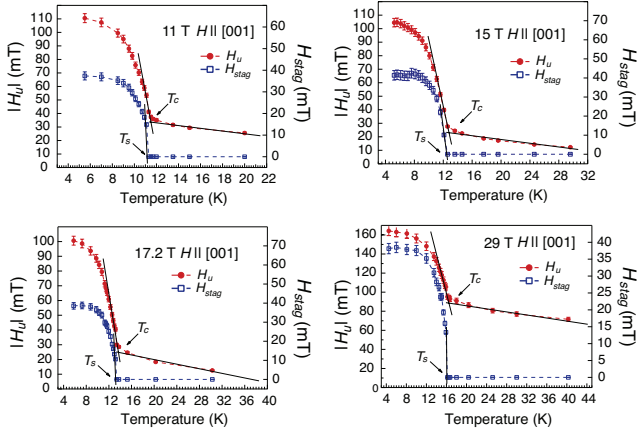


Figure 2: Temperature dependence of the uniform and staggered fields measured at various magnetic fields applied parallel to [001] crystalline axis. The uniform field data is denoted by filled circles while open squares represent staggered fields. Arrows mark transition temperature ( $T_c$ ) from PM to low temperature magnetic state, determined by the crossing points of the plotted solid lines. These  $T_c$  values are displayed in Tab. 1. Solid lines are linear fits to the data, while dashed lines are guide to the eyes.  $T_s$  marks the onset temperature for the appearance of the local staggered field.

Having described the main features of the NMR spectra, we proceed to deduce  $H - T$  phase diagram, *i.e.* transition temperatures from PM to low temperature FM and BLPS phases.

### 3.1. Low Temperature - Magnetic Phase

To determine the transition temperature ( $T_c$ ) from paramagnetic to low temperature FM state, we examine the temperature dependence of the local uniform ( $H_u$ ) and staggered ( $H_{stag}$ ) fields. We define the local uniform ( $H_u = \frac{1}{2}[\langle H_I \rangle + \langle H_{II} \rangle]$ ) and staggered ( $H_{stag} = \frac{1}{2}[\langle H_I \rangle - \langle H_{II} \rangle]$ ) fields, where the average is taken over the triplet I and II, as denoted. We note that  $H_u$  corresponds to the local field as determined by the first moment of the entire spectra.

$T_c$  from PM to low temperature FM state was determined by the crossing points of the plotted solid lines in Fig. 2. Evidently, transition temperature increases with increasing applied field, as

$H \parallel [001]$	$T_c$	$T_s$
0 T	6.3 K [9]	
7 T	9.9 K	10.2 K
9 T	10.8 K	10.6 K
11 T	11.6 K	11.3 K
15 T	13 K	12.7 K
17.2 T	13.6 K	13.4 K
29 T	16.6 K	16.2 K

Table 1: Transition temperature ( $T_c$ ) from PM to low temperature magnetic state at various applied fields.  $T_s$  marks the onset temperature for the appearance of the local staggered field. This table contains  $T_s$  values deduced from all of our NMR measurements, including our data presented here and that obtained previously in different magnetic fields from those presented in Figures. 1, 2, & 3.

summarized in Tab. 1. The increase of  $T_c$  is significant and approximately scales as the magnetic energy associated with the applied field, confirming the magnetic nature of the transition. Furthermore, we determine  $T_s$  from the onset temperature which indicates the appearance of the local staggered field. As expected, the field dependence of  $T_s$  closely follows that of  $T_c$ . This establishes that the rise of canted moments coincides with the development of LRO magnetism.

### 3.2. Intermediate Temperature - BLPS Phase

$H \parallel [001]$	$T_c$	$T^*$
0 T	6.3 K [9]	
7 T	9.9 K	11.5 K
9 T	10.8 K	12 K
11 T	11.6 K	13 K
15 T	13 K	15 K
17.2 T	13.6 K	16 K
29 T	16.6 K	20.4 K

Table 2: Transition temperature ( $T_c$ ) from PM to low temperature magnetic state at various applied fields.  $T^*$  denotes the onset temperature for breaking of local cubic symmetry. This table contains  $T_s$  and  $T^*$  values deduced from all of our NMR measurements, including our data presented here and that obtained previously in different magnetic fields from those presented in Figures. 1, 2, & 3.

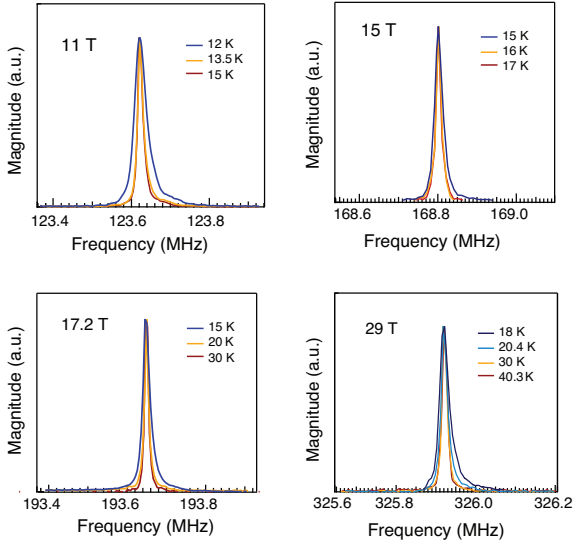


Figure 3: Temperature dependence of the  $^{23}\text{Na}$  NMR spectra measured in the PM phase at applied magnetic fields ranging from 11 T to 29 T, as denoted. This is a subset of data plotted in Fig. 1, to illustrate the appearance of notable line broadening on decreasing temperature.

Next, we proceed to identify the onset temperature for breaking of local cubic symmetry ( $T^*$ ). Breaking of local cubic symmetry is accompanied by the appearance of finite EFG at the Na site. Non-zero EFG splits the single  $^{23}\text{Na}$  line into three lines. However, for small finite values of the EFG, significant line broadening can only be detected [1]. Therefore, we identify ( $T^*$ ) as the temperature below which the width of the NMR spectral line increases notably compared to that in high temperature PM phase. The procedure is illustrated in Fig. 3. Deduced values of  $T^*$  are listed in Tab. 2. Breaking of local cubic symmetry indicates the appearance of possible orbital and/or quadrupolar ordering [3, 5]. We point out that  $T^*$  does not necessarily correspond to the true transition temperature from PM cubic to orbitally ordered BLPS state. This is because this transition could be undetectable in our experiment due to the subtlety of the effect.

The second moment of the NMR spectral line represents a quantitative measure of the width of the NMR spectral line. In Fig. 4 we plot the temperature evolution of the second moment of the NMR spectra at various applied fields. On lowering  $T$ , the second moment is dominated by

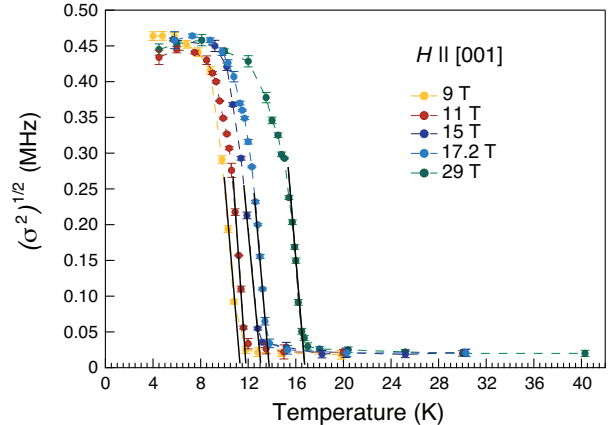


Figure 4: Temperature dependence of the second moment of the NMR spectral line, measuring the spectral width, at applied magnetic fields ranging from 9 T to 29 T, as denoted. Solid lines are linear fits to the data while dashed lines are guide to the eyes.

the increase associated with the appearance of both triplet satellite transitions and magnetism. Therefore, the temperature corresponding to the onset of rapid increase of the second moment of the NMR line, determined by the crossing points of the plotted solid lines and x-axis, does not correspond to  $T^*$  but is dominated by magnetic broadening contribution.

#### 4. Phase Diagram of $\text{Ba}_2\text{NaOsO}_6$

A phase diagram determined by our NMR measurements is plotted in Fig. 5. As magnetic field increases, BLPS phase extends over a larger temperature range.

#### 5. Summary

In conclusion, we measured the  $^{23}\text{Na}$  NMR spectra of a single crystal sample of  $\text{Ba}_2\text{NaOsO}_6$  as a function of temperature in different magnetic fields, applied parallel to [001] direction.

Clear NMR signatures of phase transition to LRO magnetic phase is identified. The transition is characterized by the sizable discontinuity of the local uniform field and abrupt appearance of the local staggered field. In addition, the onset temperature for breaking of local cubic symmetry is determined. We find that BLPS phase occupies a larger portion of the phase diagram in high fields.



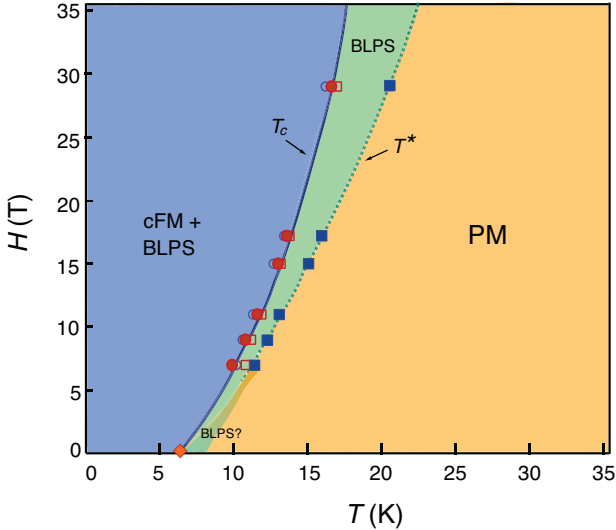


Figure 5: Sketch of the phase diagram based on our NMR measurements, both presented here and in Ref. [1]. Squares indicate onset temperature for the local cubic symmetry breaking, determined from our NMR data as explained in the text, in the paramagnetic (PM) phase. Solid circles denote  $T_c$ , transition temperature into canted ferromagnetic (cFM) phase, as deduced from the NMR data. Diamond mark  $T_c$  as determined from thermodynamic measurements in Ref. [9]. Open circles denote onset temperature for the appearance of  $H_{stag}$ , while open squares mark onset temperature for rapid increase of the NMR spectral line broadening (see Fig. 4). The solid line indicates phase transition into cFM state and also possible tetragonal-to-orthorhombic phase transition [1]. The dashed line denotes cross over to the BLPS phase, as illustrated in Fig. 3.

## 6. Acknowledgement

The study was supported in part by the the National Science Foundation DMR-1608760. The study at the NHMFL was supported by the National Science Foundation under Cooperative Agreement no. DMR95-27035, the State of Florida, and Brown University. Work at Stanford University was supported by the DOE, Office of Basic Energy Sciences, under Contract No. DE-AC02-76SF00515.

[1] L. Lu, M. Song, W. Liu, A. P. Reyes, P. Kuhns, H. O. Lee, I. R. Fisher, and V. F. Mitrović, Magnetism and local symmetry breaking in a Mott insulator with strong spin orbit interactions, *Nat. Commun.*, **8**, 14407 (2017).

- [2] G. Jackeli and G. Khaliullin, Mott Insulators in the Strong Spin-Orbit Coupling Limit: From Heisenberg to a Quantum Compass and Kitaev Models, *Phys. Rev. Lett.* **102**, 017205 (2009).
- [3] Gang Chen, Rodrigo Pereira, and Leon Balents, Exotic phases induced by strong spin-orbit coupling in ordered double perovskites, *Phys. Rev. B* **82**, 174440 (2010).
- [4] Gang Chen and Leon Balents, Spin-orbit coupling in  $d^2$  ordered double perovskites, *Phys. Rev. B*, **84**, 094420 (2011).
- [5] William Witczak-Krempa, Gang Chen, Yong Baek Kim, and Leon Balents, Correlated quantum phenomena in the strong spin-orbit regime, *Annual Review of Condensed Matter Physics*, **5**(1), 57-82 (2014).
- [6] Tyler Dodds, Ting-Pong Choy, and Yong Baek Kim, Interplay between lattice distortion and spin-orbit coupling in double perovskites, *Phys. Rev. B*, **84**, 104439 (2011).
- [7] A. Abragam, *Principles of Nuclear Magnetism*. Number 216-263. Oxford University Press, 1996.
- [8] Katharine E Stitzer, Mark D Smith, and Hans-Conrad zur Loye, Crystal growth of  $\text{Ba}_2\text{MOsO}_6$  (M=Li, Na) from reactive hydroxide fluxes, *Solid State Sciences*, **4**(3), 311 - 316 (2002).
- [9] A. S. Erickson *et al.*, Ferromagnetism in the Mott insulator  $\text{Ba}_2\text{NaOsO}_6$ , *Phys. Rev. Lett.*, **99**, 016404 (2007).